

Article

# Improved Time-Varying BLF-Based Tracking Control of a Position-Constrained Robot

Tan Zhang and Jinzhong Zhang \*

School of Electrical and Optoelectronic Engineering, West Anhui University, Lu'an 237012, China; 42000028@wxc.edu.cn

\* Correspondence: zhangjinzhongz@126.com

**Abstract:** In this work, one improved symmetric time-variant logarithmic barrier, Lyapunov function (BLF), is developed for the first time to handle the state constraint problem of nonlinear systems. It is universal in the sense that the improved barrier function is a general one that can be used not only in systems with constrained requirements but also in systems without constrained requirements, without altering the designed controller. First of all, the n-link robotic system is transformed into a kind of multi-input and multi-output (MIMO) system. Then, a trajectory tracking control scheme is designed by combining the improved time-variant logarithmic BLF with the disturbance observer to solve the problems of model uncertainty and position constraint for the robotic system. We give that under the proposed controller, all the robotic system's error vectors can trend to the equilibrium point asymptotically while the constraint conditions on the position are always met. Finally, the effectiveness of the presented scheme is indicated by completing two simulation experiment cases.

**Keywords:** adaptive control; barrier Lyapunov function; constraint control; robot; tracking control



**Citation:** Zhang, T.; Zhang, J. Improved Time-Varying BLF-Based Tracking Control of a Position-Constrained Robot. *Processes* **2023**, *11*, 2785. <https://doi.org/10.3390/pr11092785>

Academic Editors: Quanmin Zhu, Hassan el Fadil and Weicun Zhang

Received: 1 September 2023  
Revised: 12 September 2023  
Accepted: 13 September 2023  
Published: 18 September 2023



**Copyright:** © 2023 by the authors. Licensee MDPI, Basel, Switzerland. This article is an open access article distributed under the terms and conditions of the Creative Commons Attribution (CC BY) license (<https://creativecommons.org/licenses/by/4.0/>).

## 1. Introduction

For the past two decades, there has been a growing number of researchers focused on the control strategies of the MIMO systems [1–4]. The sliding mode control [5–10], for instance, is used to deal with external disturbances and modeling uncertainties of the MIMO systems due to its advantages such as fast response, insensitivity to parametric perturbations and external disturbances, online system identification is not required, and simple physical implementation, etc. Fuzzy logic systems are applied to handle system uncertain terms or model-free control problems for MIMO systems [11–13]. Neural networks are applied to system modeling and identification [14–17] like fuzzy logic systems. The uncertain terms and external disturbances of the nonlinear system are solved effectively by fuzzy approximation (universal approximation) or neural network approximation combined with adaptive control. Some adaptive feedback control methods are developed for MIMO systems with unknown dynamics and unmeasured states [18–21]. In [22–25], by manually setting the performance envelope functions of the states or errors, several excellent approaches are proposed to improve the transient and steady-state performance of the MIMO systems. However, the MIMO systems with state or error constraint problems are not studied in the above papers.

In general, there are constraints of various forms in most physical systems, such as input saturation, actuator dead-zone, safety specification, etc. However, the state constraint is the most common problem when controlling the system. Recently, utilizing barrier Lyapunov function (BLF) algorithms, several useful solutions were presented for the MIMO systems subject to constraint problems. In [26], a time-varying constraint tracking control scheme is proposed by combining an adaptive sliding mode method with a novel universal BLF for the MIMO nonlinear system. In [27], aiming at a kind of MIMO system under output constraint as well as fixed-time convergent requirements, the adaptive fixed-time constraint control approaches are presented for ensuring control

performances of tracking control systems. To handle tracking problems for MIMO systems in the presence of unmeasured states as well as time-variant state constraints, a fuzzy observer and a logarithmic BLF method are integrated into the designed controller for guarantee system states located within the constraint boundary [28]. In [29], a one-to-one nonlinear mapping is introduced to handle the system state constraint problem of strict-feedback MIMO systems while introducing a command filter to eliminate influences of “explosion of complexity” on control accuracy. Aiming at a type of MIMO non-affine nonlinear systems subject to external disturbances as well as performance constraints, a tracking control scheme is developed by utilizing the performance function, BLF, and neural networks to obtain better control performance [30]. We know that robotic systems can be transformed into a class of MIMO systems; thus, we can refer to the above schemes to complete the trajectory-tracking tasks of robotic systems.

Recently, to overcome the shortcoming that constraint requirements reduce control performances of the closed-loop systems, some effective constraint control methods have been used in robot control. In [31], aiming at the position and velocity constraint problems of the robotic manipulators with uncertain parameters, an approach in which the motion constraint problems are unified and converted into the nominal input constraint is proposed by combining neural networks to complete trajectory tracking control. Aiming at the performance requirements of practical applications for the robotic manipulators, the prescribed performance constraints are transformed into an equivalent non-constrained error to complete the high-performance tracking control [32]. In [33], by introducing a nonlinear conversion of state into the designed neuroadaptive tracking controller, the presented approach can directly handle the time-variant position as well as speed restrictions of robotic systems. In [34], an integral BLF is applied to directly handle the position restriction of a robotic manipulator. In [35–38], the time-invariant logarithmic BLF-based adaptive tracking control schemes are developed for solving the state or output restrictions of the robotic systems. For the tracking scheme for robotic manipulators, for instance, based on neural network and time-invariant logarithmic, BLF is presented to guarantee the constant output restrictions are not broken [35]. Furthermore, the constant tangent BLF is also used in dealing with the constraint requirements of the robot [39–41]. However, the constraint requirement of the physical system is generally time-varying. Time-invariant constraints are only a special situation. Therefore, in [42,43], the time-varying tangent and logarithmic BLFs are used in coping with the state restrictions of robot systems, respectively. However, the constraints in [42,43] are symmetrical. When the constraints are changed to asymmetrical, the control schemes in [42,43] will be useless. Based on this point, asymmetrical logarithmic BLF is introduced to handle the asymmetric constrained requirements of robot systems [44–46]. Further analysis of the existing literature indicates that although the logarithmic BLF can handle asymmetric constraints, it cannot be changed to an unconstrained form like the tangent BLF. In other words, the logarithmic BLF cannot work for systems with unconstrained requirements. In addition, we know that when the constrained error trends to constraint boundary, the system will provide a very large control input under the barrier function-based methods, which would reduce the control performance and lead to system input saturation and easy damage to the actuator. Recently, many effective methods have been proposed to overcome input saturation. For instance, in [47], the neural dynamic model is used to address the sudden velocity jump at the initial time; the neural dynamic model can be seen as a low-pass filter to solve unrealistic speed jumps, which helps generate smooth continuous speed signals accordingly. Smooth and continuous signals make it difficult for the system to generate excessive control inputs. In [48], a robust fault-tolerant control method is designed to deal with the adverse effect of the actuator saturation. The saturation nonlinearity is described by introducing a novel dead-zone model, and an adaptive method is used to compensate for the nondifferentiable integral term of the dead-zone model. In [49], an auxiliary dynamics system is constructed to address the actuator saturation issue in tracking control of the quadrotor UAV with external disturbances. The controller dealing with actuator saturation can ensure the tracking

errors can trend to small neighborhoods around zero within a finite time. A command filtering-based fuzzy control is proposed to cope with saturation nonlinearity input in uncertain MIMO nonlinear systems [50]. There are many approaches to deal with the actuator saturation issues of the nonlinear system. However, the key issue of this article is to design a novel logarithmic barrier function to constrain the system state. In the future, the saturation control method will be introduced to deal with the actuator saturation problem caused by constraint control based on barrier function.

Based on the above discussions, this article tries to modify the existing logarithmic barrier function so that it can work simultaneously for systems with constrained and unconstrained requirements. The improved logarithmic barrier function-based tracking control scheme of a robotic system subject to time-variant position constraints is studied, and the robotic system is transformed into a type of MIMO system. The contribution points of this article are listed below.

- (1) On the basis of the existing logarithmic barrier function, we multiply the original barrier function with the constraint boundary to obtain an improved barrier function for dealing with the symmetric time-varying constraint requirements of robot systems for the first time. The proposed barrier function can be used for controller design of systems subject to partial state constraints.
- (2) Different from the existing logarithmic BLFs [35–38,43–46], the improved BLF-based control scheme is a universal one that can be used simultaneously in systems with constraint requirements and without constraint requirements, without altering the designed controller. In addition, the inequality condition for the proposed barrier function is also given to provide a basis for the subsequent proof of system stability. At the same time, it has been theoretically proven that the proposed barrier function can directly design the controller for unconstrained systems.
- (3) It can be proven that the system's error signals can trend to zero asymptotically, and the position constraint boundary is never violated under the proposed controller. In the end, the effectiveness of the presented scheme is indicated by performing three simulation cases.

The remaining work is listed below. The definition and Theorem of the modified barrier function, as well as the useful Lemma, are given in Section 2. Section 3 describes the design process of the robotic system's control scheme as well as stability analysis. Section 4 completes two simulation examples that demonstrate the effectiveness, as well as the universality, of the proposed approach. In the end, the conclusion of this paper is summarized in Section 5.

## 2. Problem Statements and Preliminaries

### 2.1. Improved Time-Varying Barrier Function

**Definition 1.** An improved time-varying logarithmic BLE, which can work for systems with or without constraint needs, is presented for the first time as

$$V_t(k(t), e(t)) = \frac{k^2(t)}{2} \log \frac{k^2(t)}{k^2(t) - e^2(t)} \quad (1)$$

where  $e(t) = x - x_d$  denotes the system's constrained error, the desired trajectory is set as  $x_d$ , and  $k(t) > 0$  represents the time-varying constraint function,  $\log$  is the natural logarithm. It is obvious from the definition of  $V_t(k(t), e(t))$  that the functional  $V_t(k(t), e(t))$  is positive continuous, differentiable, and radially unbounded as  $|e(t)| \rightarrow k(t)$  over the set  $\Omega_t := \{e(t), |e(t)| < k(t)\}$ .

**Theorem 1.** The improved barrier functional  $V_t(k(t), e(t))$  constructed in (1) over the set  $\Omega_t$  meets the following condition

$$\frac{e^2(t)}{2} \leq V_t(k(t), e(t)) \leq \frac{1}{2} \frac{k^2(t)e^2(t)}{k^2(t) - e^2(t)} \quad (2)$$

**Proof of Theorem 1.** Step 1: In this step, we will indicate that the inequality on the left side of (2) holds. Firstly, the following auxiliary function is defined as

$$f(e) = \frac{k^2(t)}{2} \log \frac{k^2(t)}{k^2(t) - e^2(t)} - \frac{e^2(t)}{2} \quad (3)$$

Taking the derivative of (3) with respect to the constrained error  $e(t)$ , we get

$$\begin{aligned} \frac{\partial f(e)}{\partial e(t)} &= \frac{k^2(t)e(t)}{k^2(t) - e^2(t)} - e(t) \\ &= \frac{e^3(t)}{k^2(t) - e^2(t)} \end{aligned} \quad (4)$$

From (4), we know that  $\frac{\partial f(e)}{\partial e(t)} < 0$  holds when  $e(t) < 0$  and  $\frac{\partial f(e)}{\partial e(t)} > 0$  is true when  $e(t) > 0$  over the set  $\Omega_t$ . Additionally,  $f(e) = 0$  and  $e(t) = 0$ . Therefore, we can deduce that the inequality  $\frac{e^2(t)}{2} \leq V_t(k(t), e(t))$  always holds over the set  $\Omega_t$ .

Step 2: In this step, the inequality on the right side of (2) will be proven. Similar to step 1, the second auxiliary function is constructed as

$$g(e) = \frac{1}{2} \frac{k^2(t)e^2(t)}{k^2(t) - e^2(t)} - \frac{k^2(t)}{2} \log \frac{k^2(t)}{k^2(t) - e^2(t)} \quad (5)$$

Taking the derivative of the above equation yields

$$\begin{aligned} \frac{\partial g(e)}{\partial e(t)} &= \frac{k^4(t)e(t)}{(k^2(t) - e^2(t))^2} - \frac{k^2(t)e(t)}{k^2(t) - e^2(t)} \\ &= \frac{k^2(t)e^3(t)}{(k^2(t) - e^2(t))^2} \end{aligned} \quad (6)$$

It is obvious from (6) that  $\frac{\partial g(e)}{\partial e(t)} < 0$  is true as  $e(t) < 0$  and  $\frac{\partial g(e)}{\partial e(t)} > 0$  holds as  $e(t) > 0$  over the set  $\Omega_t$ . Furthermore, by means of (5),  $g(e) = 0$  can be obtained as  $e(t) = 0$ . Thus, it can be inferred that the condition  $V_t(k(t), e(t)) \leq \frac{1}{2} \frac{k^2(t)e^2(t)}{k^2(t) - e^2(t)}$  is always true over the set  $\Omega_t$ .  $\square$

**Remark 1.** Almost all logarithmic barrier functions used in existing articles [35–38,43–46] have the following two types of forms, that is, time-varying and time-invariant types

$$V = \frac{1}{2} \log \frac{k^2(t)}{k^2(t) - e^2(t)} \quad \text{or} \quad = \frac{1}{2} \log \frac{k^2}{k^2 - e^2(t)} \quad (7)$$

When the systems are without constraint requirements, that is,  $k$  and  $k(t) \rightarrow \infty$ , we have  $V \rightarrow 0$ . Thus, the above logarithmic barrier functions cannot work for general systems with no-constraint needs. In light of Theorem 1, we know that the improved logarithmic barrier function meets the condition  $\frac{e^2(t)}{2} \leq V_t(t) \leq \frac{1}{2} \frac{k^2(t)e^2(t)}{k^2(t) - e^2(t)}$ . Subsequently, as  $k(t) \rightarrow \infty$ , the limit on the right-hand of (2) is given as

$$\lim_{k(t) \rightarrow \infty} \frac{1}{2} \frac{k^2(t)e^2(t)}{k^2(t) - e^2(t)} = \frac{1}{2} e^2(t) \quad (8)$$

In terms of the Squeeze Theorem (Sandwich Theorem), one gets

$$\lim_{k(t) \rightarrow \infty} \left( V_t(k(t), e(t)) = \frac{k^2(t)}{2} \log \frac{k^2(t)}{k^2(t) - e^2(t)} \right) = \frac{e^2(t)}{2} \quad (9)$$

Therefore, the improved logarithmic barrier function  $V_t(t)$  presented in this work can be transformed into a general quadratic type Lyapunov function, which works for systems without constraint requirements. It can be said that the improved logarithmic barrier function has a more universal and wide application scope than the existing logarithmic barrier functions (7).

**Lemma 1.** In terms of article [51], we construct the open set  $N := R^l \times Z \in R^{l+1}$  as well as  $Z := \{z \in R : |z| < k(t)\} \subset R$  with  $k(t)$  being the constraint boundary and any positive function. Aiming at the following system

$$\dot{\eta} = h(\eta, t) \quad (10)$$

with states of the system  $\eta := [\omega, z]^T \in N$  as well as functional  $h : R_+ \times N \rightarrow R^{l+1}$  being locally Lipschitz in  $\eta$ , uniform in time,  $t$ , over set  $R_+ \times N$ , and piecewise continuous over time  $t$ . Supposing we can construct the continuous differential as well as positive definite functions  $U : R^l \rightarrow R_+$  and  $V_1 : z \rightarrow R_+$ , such that

$$V_1(z) \rightarrow \infty \quad \text{as} \quad |z| \rightarrow k(t) \quad (11)$$

$$\gamma_1(\|\omega\|) \leq U(\omega) \leq \gamma_2(\|\omega\|) \quad (12)$$

with  $\gamma_1$  and  $\gamma_2$  representing class  $k_\infty$  functions. Constructing a Lyapunov function candidate as  $V(\eta) = V_1(z) + U(\omega)$  and supposing that the initial condition  $z(0)$  locates within the set  $|z| < k(t)$ , taking the derivative of  $V$  over the set  $|z| < k(t)$ , if the following inequality is true

$$\dot{V} = \frac{\partial V}{\partial \eta} h \leq -\mu V \leq 0, \eta \in N \quad (13)$$

with  $\mu$  being a positive constant, then we can conclude that  $\omega$  is bounded and  $z$  maintains in set  $|z| < k(t)$ ,  $\forall t \in [0, \infty)$ .

**Remark 2.** In view of Lemma 1, it can be learned that we can divide states of the systems with partial state constraints into constrained and unconstrained ones. Then, we need to construct a barrier function for the constrained state to ensure that the constraint conditions are always met. At the same time, quadratic form Lyapunov functions are constructed for unconstrained states to guarantee the system's stability.

## 2.2. System Formulation

In this work, a robotic system with  $n$ -degrees is depicted as follows [37,52]

$$M_0(q)\ddot{q} + C_0(q, \dot{q})\dot{q} + G_0(q) = \tau(t) + f_{s\_un} \quad (14)$$

with  $f_{s\_un} = -\Delta C(q, \dot{q})\dot{q} - \Delta M(q)\ddot{q} - \Delta G(q) - J^T(q)f(t)$  representing the robotic system's uncertain terms,  $J^T(q)$  being the Jacobian matrix,  $f(t)$  denoting the unknown force that is generated by the contact between the end of the robot and the external environment,  $M_0(q) \in R^{n \times n}$  standing for the inertia matrix of the robotic system and the condition  $M_0(q) = M_0^T(q) > 0$  being met,  $G_0(q) \in R^n$  and  $C_0(q, \dot{q})\dot{q} \in R^n$  standing for the gravitational matrix and the Coriolis-centripetal torque, respectively,  $q$  standing for the positions of the robotic joint as well as their velocity, and acceleration being represented, respectively, by  $\dot{q}$  and  $\ddot{q}$ , control inputs of each robotic arms being denoted by  $\tau(t)$ .

### 2.3. Basic Assumptions and System Transformation

Next, the robotic system with n-degrees is changed to a MIMO system by using the coordinate conversion

$$\begin{cases} x_1 = q \\ x_2 = \dot{q} \end{cases} \quad (15)$$

The robotic system can be depicted as follows

$$\begin{cases} \dot{x}_1 = x_2 \\ \dot{x}_2 = M_0^{-1}(x_1)[\tau(t) + f_{un} - C_0(x_1, x_2)x_2 - G_0(x_1)] \\ y = x_1 \end{cases} \quad (16)$$

The control objective in this work attempts to design the tracking controller of uncertain robotic systems based on the improved time-variant symmetric logarithmic barrier function to make the position vectors  $y = x_1 = q = [q_1, q_2, \dots, q_n]^T$  track reference trajectories  $x_d = q_d = [x_{d1}, x_{d2}, \dots, x_{dn}]^T$  successfully. All the robotic system's error signals are asymptotically stable, and the constraint conditions are always met, namely  $|x_1| < k_c(t) = [k_{c1}(t), k_{c2}(t), \dots, k_{cn}(t)]^T$ .

**Assumption 1.** The uncertain terms of the system are bounded, differentiable, and slowly varying, namely

$$\begin{aligned} |f_{un}| &\leq F_m, F_m > 0 \\ \dot{f}_{un} &\approx 0 \end{aligned} \quad (17)$$

**Assumption 2.** The matrix  $M_0(x_1)$  is symmetric and invertible, and the matrixes  $M_0^{-1}(x_1)$ ,  $C_0(x_1, x_2)$ , and  $G_0(x_1)$  are bounded.

**Assumption 3.** The reference trajectories  $x_d$  as well as their derivatives  $\dot{x}_d$  are bounded.

**Assumption 4.** There exist the constant vectors  $X_1$  satisfying  $X_1 < k_c(t), \forall t \geq 0$  with  $k_c(t)$  being the constraint condition of the position state, such that  $|x_d| \leq X_1$ . Set the constraint boundary of the position tracking error to be  $k_q(t) = k_c(t) - X_1$ .

**Remark 3.** It should be noted that Assumptions 1–4 are made for subsequent stability analysis. Assumptions 1–3 are relatively fundamental and reasonable because the uncertain terms, system matrixes, and desired trajectory of an actual robot are often bounded in practice. The boundedness and invertibility of the inertia matrix are the keys to ensuring the smooth derivation of the control law. Assumption 4 provides the basis for selecting the desired trajectory; that is, in order for constraint control to be successful, the desired trajectory also needs to be maintained within the constraint boundary  $k_c(t)$ .

### 3. Design Process of Controller and Stability Analysis

One improved time-varying logarithmic barrier function is applied to designing the tracking controller for the uncertain robotic arms in this section. First of all, the position as well as velocity tracking errors are defined, respectively, as  $e_1 = [e_{11}, e_{12}, \dots, e_{1n}]^T = x_1 - x_d$  and  $e_2 = [e_{21}, e_{22}, \dots, e_{2n}]^T = x_2 - \alpha$ , where  $\alpha$  stands for the desired velocity that will be designed later. To complete the position constraint control, we constructed the following improved time-varying logarithmic BLF.

$$V_1 = \sum_{i=1}^n \frac{k_{qi}^2(t)}{2} \log \frac{k_{qi}^2(t)}{k_{qi}^2(t) - e_{1i}^2} \quad (18)$$

where  $k_q(t) = k_c(t) - X_1 = [k_{q1}(t), k_{q2}(t), \dots, k_{qn}(t)]^T, |x_d| \leq X_1$ .

Taking the derivative of  $V_1$  yields

$$\begin{aligned}\dot{V}_1 &= \sum_{i=1}^n \frac{\partial V_1}{\partial e_{1i}} \frac{de_{1i}}{dt} + \sum_{i=1}^n \frac{\partial V_1}{\partial k_{qi}(t)} \frac{dk_{qi}(t)}{dt} \\ &= \sum_{i=1}^n \frac{k_{qi}^2(t)e_{1i}}{k_{qi}^2(t)-e_{1i}^2} \dot{e}_{1i} \\ &\quad + \sum_{i=1}^n \left( k_{qi}(t) \log \frac{k_{qi}^2(t)}{k_{qi}^2(t)-e_{1i}^2} - \frac{k_{qi}(t)e_{1i}^2}{k_{qi}^2(t)-e_{1i}^2} \right) \dot{k}_{qi}(t)\end{aligned}\quad (19)$$

According to the definition of  $e_1$  and differentiating  $e_1$ , with respect to time, we get

$$\begin{aligned}\dot{e}_1 &= \dot{x}_1 - \dot{x}_d \\ &= e_2 + \alpha - \dot{x}_d \\ \dot{e}_{1i} &= e_{2i} + \alpha_i - \dot{x}_{di}\end{aligned}\quad (20)$$

By means of the backstepping method, the desired velocity  $\alpha$  is developed as

$$\begin{aligned}\alpha &= \dot{x}_d - A - B \\ \alpha_i &= \dot{x}_{di} - A_{1i} - B_{1i}\end{aligned}\quad (21)$$

where

$$A = \begin{bmatrix} A_{11} \\ A_{12} \\ \dots \\ A_{1n} \end{bmatrix} = \begin{bmatrix} k_{11}e_{11} \\ k_{12}e_{12} \\ \dots \\ k_{1n}e_{1n} \end{bmatrix}\quad (22)$$

$$B = [B_{11}, B_{12}, \dots, B_{1n}]^T = K_{dot} B' \quad (23)$$

and

$$B' = \begin{bmatrix} \frac{k_{q1}^2(t)-e_{11}^2}{k_{q1}^2(t)} \left( \frac{k_{q1}(t)}{e_{11}} \log \frac{k_{q1}^2(t)}{k_{q1}^2(t)-e_{11}^2} - \frac{k_{q1}(t)e_{11}}{k_{q1}^2(t)-e_{11}^2} \right) \\ \frac{k_{q2}^2(t)-e_{12}^2}{k_{q2}^2(t)} \left( \frac{k_{q2}(t)}{e_{12}} \log \frac{k_{q2}^2(t)}{k_{q2}^2(t)-e_{12}^2} - \frac{k_{q2}(t)e_{12}}{k_{q2}^2(t)-e_{12}^2} \right) \\ \dots \\ \frac{k_{qn}^2(t)-e_{1n}^2}{k_{qn}^2(t)} \left( \frac{k_{qn}(t)}{e_{1n}} \log \frac{k_{qn}^2(t)}{k_{qn}^2(t)-e_{1n}^2} - \frac{k_{qn}(t)e_{1n}}{k_{qn}^2(t)-e_{1n}^2} \right) \end{bmatrix}\quad (24)$$

$$K_{dot} = \text{diag}(\dot{k}_{q1}(t), \dot{k}_{q2}(t), \dots, \dot{k}_{qn}(t)) \quad (25)$$

and  $k_{1i} > 0$  is the control gain.

**Remark 4.** In view of (24), it can be seen that there are tracking errors  $e_{1i}$  in the denominator of the virtual control law  $\alpha$  that may cause singularity problems. However, according to L' Hopital's rule, we take the limit as  $e_{1i}$  approaches zero.

$$\lim_{e_{1i} \rightarrow 0} \frac{k_{qi}(t)}{e_{1i}} \log \frac{k_{qi}^2(t)}{k_{qi}^2(t)-e_{1i}^2} = \frac{2k_{qi}(t)e_{1i}}{k_{qi}^2(t)-e_{1i}^2}, i = 1, 2 \dots n \quad (26)$$

Therefore, the virtual position constraint control law  $\alpha$  is well-defined.

Substituting (20) into (19), we get

$$\begin{aligned}\dot{V}_1 &= \sum_{i=1}^n \frac{k_{qi}^2(t)e_{1i}}{k_{qi}^2(t)-e_{1i}^2} (e_{2i} + \alpha_i - \dot{x}_{di}) \\ &\quad + \sum_{i=1}^n \left( k_{qi}(t) \log \frac{k_{qi}^2(t)}{k_{qi}^2(t)-e_{1i}^2} - \frac{k_{qi}(t)e_{1i}^2}{k_{qi}^2(t)-e_{1i}^2} \right) \dot{k}_{qi}(t)\end{aligned}\quad (27)$$

Considering (21)–(25) and (27) becomes

$$\begin{aligned}
 \dot{V}_1 &= \sum_{i=1}^n \frac{k_{qi}^2(t)e_{1i}}{k_{qi}^2(t) - e_{1i}^2} (e_{2i} - A_{1i} - B_{1i}) \\
 &+ \sum_{i=1}^n \left( k_{qi}(t) \log \frac{k_{qi}^2(t)}{k_{qi}^2(t) - e_{1i}^2} - \frac{k_{qi}(t)e_{1i}^2}{k_{qi}^2(t) - e_{1i}^2} \right) \dot{k}_{qi}(t) \\
 &= \sum_{i=1}^n \frac{k_{qi}^2(t)e_{1i}}{k_{qi}^2(t) - e_{1i}^2} e_{2i} - \sum_{i=1}^n \frac{k_{1i}k_{qi}^2(t)e_{1i}^2}{k_{qi}^2(t) - e_{1i}^2} \\
 &- \sum_{i=1}^n e_{1i} \dot{k}_{qi}(t) \left( \frac{k_{qi}(t)}{e_{1i}} \log \frac{k_{qi}^2(t)}{k_{qi}^2(t) - e_{1i}^2} - \frac{k_{qi}(t)e_{1i}}{k_{qi}^2(t) - e_{1i}^2} \right) \\
 &+ \sum_{i=1}^n \left( k_{qi}(t) \log \frac{k_{qi}^2(t)}{k_{qi}^2(t) - e_{1i}^2} - \frac{k_{qi}(t)e_{1i}^2}{k_{qi}^2(t) - e_{1i}^2} \right) \dot{k}_{qi}(t) \\
 &= - \sum_{i=1}^n \frac{k_{1i}k_{qi}^2(t)e_{1i}^2}{k_{qi}^2(t) - e_{1i}^2} + \sum_{i=1}^n \frac{k_{qi}^2(t)e_{1i}}{k_{qi}^2(t) - e_{1i}^2} e_{2i}
 \end{aligned} \tag{28}$$

By means of (16), taking the derivative of  $e_2$  yields

$$\dot{e}_2 = M_0^{-1}(x_1)[\tau(t) + f_{un} - C_0(x_1, x_2)x_2 - G_0(x_1)] - \dot{\alpha} \tag{29}$$

Due to the presence of uncertain terms in the derivative of velocity tracking errors. Thus, a disturbance observer is introduced to complete estimation and compensation for them:

$$\begin{cases} \dot{\hat{f}}_{un} = \delta_f + k_f M_0 x_2 \\ \dot{\delta}_f = -k_f \delta_f - k_f [\tau(t) - C_0 x_2 - G_0 + k_f M_0 x_2] \end{cases} \tag{30}$$

where  $k_f = \text{diag}(k_{f11}, k_{f22}, \dots, k_{fnn})$  is the observer parameter,  $\delta_f \in \mathbb{R}^n$  presents the observer state.  $\hat{f}_{un}$  is the estimated value of  $f_{un}$ , the estimating error is described as  $\tilde{f}_{un} = f_{un} - \hat{f}_{un}$ .

Subsequently, the second Lyapunov function is selected

$$V_2 = V_1 + \frac{1}{2} e_2^T M_0 e_2 + \frac{1}{2} \tilde{f}_{un}^T \tilde{f}_{un} \tag{31}$$

Differentiating (31) yields

$$\dot{V}_2 = - \sum_{i=1}^n \frac{k_{1i}k_{qi}^2(t)e_{1i}^2}{k_{qi}^2(t) - e_{1i}^2} + \sum_{i=1}^n \frac{k_{qi}^2(t)e_{1i}}{k_{qi}^2(t) - e_{1i}^2} e_{2i} + e_2^T M_0 \dot{e}_2 + \tilde{f}_{un}^T \dot{\tilde{f}}_{un} \tag{32}$$

According to Lyapunov stability theory, the controller is designed as

$$\begin{aligned}
 \tau(t) &= C_0 x_2 + G_0 + M_0 \dot{\alpha} - \hat{f}_{un} - K_2 e_2 \\
 &- \left[ \frac{k_{q1}^2(t)e_{11}}{k_{q1}^2(t) - e_{11}^2}, \frac{k_{q2}^2(t)e_{12}}{k_{q2}^2(t) - e_{12}^2}, \dots, \frac{k_{qn}^2(t)e_{1n}}{k_{qn}^2(t) - e_{1n}^2} \right]^T
 \end{aligned} \tag{33}$$

with  $K_2 = \text{diag}(k_{21}, k_{22}, \dots, k_{2n})$  being the positive definite control parameter.

**Theorem 2.** Considering a robotic system with  $n$ -degrees subject to position constraints as well as unknown uncertain terms and supposing Assumptions 1–4 are always met, and the initial positions are located within  $|e_{1i}(0)| < k_{qi}(0)$ . Then, the robotic system's error signals can trend asymptotically to zero, and the position constraint boundaries are never violated under the proposed controller.

**Proof of Theorem 2.** Substituting (29) into (32) yields

$$\begin{aligned} \dot{V}_2 &= -\sum_{i=1}^n \frac{k_{1i}k_{qi}^2(t)e_{1i}^2}{k_{qi}^2(t)-e_{1i}^2} + \sum_{i=1}^n \frac{k_{qi}^2(t)e_{1i}}{k_{qi}^2(t)-e_{1i}^2} e_{2i} \\ &\quad + e_2^T([\tau(t) + f_{s\_un} - C_0(x_1, x_2)x_2 - G_0(x_1)] - M_0\dot{\alpha}) + \tilde{f}_{un}^T \tilde{f}_{un} \end{aligned} \tag{34}$$

Differentiating  $\hat{f}_{un}$  yields

$$\begin{aligned} \dot{\hat{f}}_{un} &= \dot{\delta}_f + k_f M_0 \dot{x}_2 \\ &= -k_f \delta_f - k_f (k_f M_0 x_2) + k_f f_{un} \\ &= -k_f (\delta_f + k_f M_0 x_2) + k_f f_{un} \\ &= -k_f \hat{f}_{un} + k_f f_{un} = k_f \tilde{f}_{un} \end{aligned} \tag{35}$$

Considering (33) and (35), (34) can be rewritten as

$$\begin{aligned} \dot{V}_2 &= -\sum_{i=1}^n \frac{k_{1i}k_{qi}^2(t)e_{1i}^2}{k_{qi}^2(t)-e_{1i}^2} - e_2^T K_2 e_2 + e_2^T \tilde{f}_{un} - \tilde{f}_{un}^T k_f \tilde{f}_{un} \\ &\leq -\sum_{i=1}^n \frac{k_{1i}k_{qi}^2(t)e_{1i}^2}{k_{qi}^2(t)-e_{1i}^2} - e_2^T \left(K_2 - \frac{1}{2}I_n\right) e_2 - \tilde{f}_{un}^T \left(k_f - \frac{1}{2}I_n\right) \tilde{f}_{un} \end{aligned} \tag{36}$$

with  $I_n = \text{diag}(1, 1, \dots, 1)_{n \times n}$  representing the identity matrix.

The coefficients  $K_2$  and  $k_f$  are set to meet the following conditions:

$$\begin{aligned} \lambda_{\min} \left(K_2 - \frac{1}{2}I_n\right) &> 0 \\ \lambda_{\min} \left(k_f - \frac{1}{2}I_n\right) &> 0 \end{aligned} \tag{37}$$

By means of Theorem 1, (36) can be rewritten as

$$\begin{aligned} \dot{V}_2 &\leq -\sum_{i=1}^n 2k_{1i} \frac{k_{qi}^2(t)}{2} \log \frac{k_{qi}^2(t)}{k_{qi}^2(t)-e_{1i}^2} - e_2^T \left(K_2 - \frac{1}{2}I_n\right) e_2 - \tilde{f}_{un}^T \left(k_f - \frac{1}{2}I_n\right) \tilde{f}_{un} \\ &\leq -\rho V_2 \leq 0 \end{aligned} \tag{38}$$

where

$$\rho = \min \left( 2k_{1i}, \frac{2\lambda_{\min} \left(K_2 - \frac{1}{2}I_n\right)}{\lambda_{\max} (M_0)}, 2\lambda_{\min} \left(k_f - \frac{1}{2}I_n\right) \right) \tag{39}$$

In light of Lemma 1 and (38), we learned that the errors  $e_2$  and  $\tilde{f}_{un}$  are bounded, and the position errors meet conditions  $|e_{1i}(t)| < k_{qi}(t)$  all the time. Next, we will use mathematical methods to further describe Theorem 2. Seeking the solution of the differential Equation (38), we have

$$0 \leq V_2 \leq V_2(0)e^{-\rho t} \tag{40}$$

In terms of (18) and (31), we have

$$V_2 = \sum_{i=1}^n \frac{k_{qi}^2(t)}{2} \log \frac{k_{qi}^2(t)}{k_{qi}^2(t)-e_{1i}^2} + \frac{1}{2}e_2^T M_0 e_2 + \frac{1}{2}\tilde{f}_{un}^T \tilde{f}_{un} \tag{41}$$

In view of (40), we have

$$\frac{k_{qi}^2(t)}{2} \log \frac{k_{qi}^2(t)}{k_{qi}^2(t)-e_{1i}^2} \leq V_2(0)e^{-\rho t} \leq \bar{V}_2 \tag{42}$$

where  $\bar{V}_2$  is bounded positive constant.

Using (42), we can obtain

$$e_{1i}^2 \leq k_{qi}^2(t) \left( 1 - e^{\frac{-2V_2}{k_{qi}^2(t)}} \right) < k_{qi}^2(t) \quad (43)$$

Thus, we have  $|e_{1i}| < k_{qi}(t)$ . In light of Assumption 4 and  $k_q(t) = k_c(t) - X_1$ ,  $|x_d| \leq X_1$ , the position constraint condition  $|x_1| < k_c(t)$  are met at all time. By means of Theorem 1, we can further obtain

$$\frac{e_{1i}^2}{2} \leq \frac{k_{qi}^2(t)}{2} \log \frac{k_{qi}^2(t)}{k_{qi}^2(t) - e_{1i}^2} \leq V_2(0)e^{-\rho t} \quad (44)$$

Considering (40), (41), and (44), the following inequalities hold

$$\begin{aligned} |e_1| &\leq \sqrt{2V_2(0)e^{-\rho t}} \\ |e_2| &\leq \sqrt{\frac{2V_2(0)e^{-\rho t}}{\lambda_{\min}(M_0)}} \\ |\tilde{f}_{un}| &\leq \sqrt{2V_2(0)e^{-\rho t}} \end{aligned} \quad (45)$$

To sum up, the robotic system's error signals can trend exponentially asymptotically to zero, and position constraint boundaries are always met under the proposed method.  $\square$

**Remark 5.** By means of the proof of Theorem 2, it can arrive at the conclusion that the proposed controller based on the improved time-varying logarithmic barrier function can not only ensure the constraint conditions are always met but also ensure the system's constrained errors are asymptotically stable to the equilibrium point. The logarithmic function used in the existing literature [35–38,43–46] can only guarantee that the system's constrained error trends to a specific region. It can be said that the presented method is more general and advantageous.

**Remark 6.** In addition to the barrier Lyapunov function, there are also methods for state constraint control of the nonlinear system. For example, the control barrier function in [53]. In [53], the constraint boundary is dependent on the control input and states of the system. This constraint boundary is closer to the limit space of the actual system. However, this article focuses on designing new barrier functions, therefore only artificially setting a boundary condition for the robot state to verify the effectiveness of the proposed barrier function. In future works, the boundary condition that depends on state and control input will be focused on.

**Remark 7.** Control barrier functions as a new safety control method that aims to guarantee safety by limiting the control input such that the system state is located within a set safe range [53–55]. In [55], a controller is proposed based on a disturbance observer to estimate the effect of the disturbance on safety; the estimation value and control barrier function are used to achieve provably safe dynamic behavior. The form of the observer is similar to that of the observer in this article, and the observers are all used to estimate the unknown terms of the system. In the control barrier function method, the safety condition depends on control input and states. This safety condition is very practical and effective in engineering control. However, the constraint condition is artificially set to verify the effectiveness of the novel logarithmic barrier function proposed in this paper. The constraint condition setting did not take into account the actual safety space of the robot. We hope to consider more complex constraint boundary-setting methods in future research work.

#### 4. Simulation and Discussion

In this section, a robotic system with two degrees is applied to simulation experiments to indicate the feasibility of the presented method in this paper. The joint mass and length

of the simulated robot object are represented by  $m_i$  and  $l_i$ ,  $i = 1, 2$ , respectively. To facilitate the establishment of the robot mathematical model, we suppose that equivalent masses are located at the end of each link. The displacement between joint  $i - 1$  and the centroid of link  $i$  is denoted by  $r_i$ .

The joint position vector is set as

$$q = \begin{bmatrix} q_1 \\ q_2 \end{bmatrix} = \begin{bmatrix} \theta_1 \\ \theta_2 \end{bmatrix} \quad (46)$$

The relevant matrixes of the two-degree robot are given as [37,52]

$$M_0(q) = \begin{bmatrix} M_{11} & M_{12} \\ M_{21} & M_{22} \end{bmatrix} \quad (47)$$

$$C_0(q, \dot{q}) = \begin{bmatrix} C_{11} & C_{12} \\ C_{21} & C_{22} \end{bmatrix} \quad (48)$$

$$G_0(q) = [G_{11} \quad G_{12}]^T \quad (49)$$

$$J(q) = \begin{bmatrix} -(l_1 \sin q_1 + l_2 \sin(q_1 + q_2)) & -l_2 \sin(q_1 + q_2) \\ l_1 \cos q_1 + l_2 \cos(q_1 + q_2) & l_2 \cos(q_1 + q_2) \end{bmatrix} \quad (50)$$

and

$$\begin{aligned} M_{11} &= m_1 r_1^2 + m_2 (l_1^2 + r_2^2 + 2l_1 r_2 \cos q_2) + I_1 + I_2 \\ M_{12} &= m_2 (r_2^2 + l_1 r_2 \cos q_2) + I_2 \\ M_{21} &= m_2 (r_2^2 + l_1 r_2 \cos q_2) + I_2 \\ M_{22} &= m_2 r_2^2 + I_2 \\ C_{11} &= -m_2 l_1 r_2 \dot{q}_2 \sin q_2 \\ C_{12} &= -m_2 l_1 r_2 (\dot{q}_2 + \dot{q}_1) \sin q_2 \\ C_{21} &= m_2 l_1 r_2 \dot{q}_1 \sin q_2 \\ C_{22} &= 0 \\ G_{11} &= (m_1 r_2 + m_2 l_1) g \cos q_1 + m_2 r_2 g \cos(q_1 + q_2) \\ G_{12} &= m_2 r_2 g \cos(q_1 + q_2). \end{aligned} \quad (51)$$

Referring to papers [37,52], the main parameters of the robot with two degrees are set as:  $m_1 = 2$  kg,  $m_2 = 0.85$  kg,  $l_1 = 0.35$  m,  $l_2 = 0.31$  m,  $r_1 = \frac{1}{2}l_1$ ,  $r_2 = \frac{1}{2}l_2$ ,  $I_1 = \frac{1}{4}m_1 l_1^2$ ,  $I_2 = \frac{1}{4}m_2 l_2^2$ , and  $g = 9.81$  m/s<sup>2</sup>.

The initial joint position vectors are presumed as

$$\begin{cases} q_1(0) = -0.08, q_2(0) = 0.05 \\ \dot{q}_1(0) = 0, \dot{q}_2(0) = 0 \end{cases} \quad (52)$$

The reference trajectories are set as

$$x_d = [0.14 \sin(t), 0.14 \cos(t)]^T \quad (53)$$

The uncertain terms of the robotic system are presumed as

$$f_{un} = M_0[0.3 \sin(t), 0.3 \cos(t)]^T + C_0[0.3 \cos(0.5t), 0.3 \sin(0.5t)]^T \quad (54)$$

In order to determine the feasibility of the presented approach, the numerical simulations are separated into two cases. In the first case, when the constraint boundary is changed into a time-invariant situation. The controller (21), without compensation for uncertain terms, can be rewritten as

$$\begin{aligned} \alpha &= \dot{x}_d - A \\ \alpha_i &= \dot{x}_{di} - A_{1i} \end{aligned} \quad (55)$$

where

$$A = \begin{bmatrix} A_{11} \\ A_{12} \\ \dots \\ A_{1n} \end{bmatrix} = \begin{bmatrix} k_{11}e_{11} \\ k_{12}e_{12} \\ \dots \\ k_{1n}e_{1n} \end{bmatrix} \quad (56)$$

and (33) can be rewritten as

$$\tau(t) = C_0x_2 + G_0 + M_0\dot{\alpha} - K_2e_2 - \left[ \frac{k_{q1}^2e_{11}}{k_{q1}^2 - e_{11}^2}, \frac{k_{q2}^2e_{12}}{k_{q2}^2 - e_{12}^2}, \dots, \frac{k_{qn}^2e_{1n}}{k_{qn}^2 - e_{1n}^2} \right]^T \quad (57)$$

In the second case, the controllers (21) and (33) are applied to indicate that the improved time-variant logarithmic barrier function is feasible.

In the third case, we set the constraint boundary to infinite as  $k_{q1}(t) = k_{q2}(t) = 10^8$  to verify that the proposed method can be applied to address the tracking control issue of the unconstrained system.

**Remark 8.** In order to verify the effectiveness of the proposed method and achieve better control effects in the different control conditions, we set up three different simulation scenarios: (1) The constraint boundary is time-invariant. (2) The constraint boundary is time-varying. (3) The constraint boundary is set to be infinite. In the condition (1), we choose controller (57) to deal with time-invariant constraint issues. The controller (33) is used to address the time-varying constraint problems in condition (2). When the constraint condition  $k_{qi}(t) \rightarrow \infty$  in condition (3), the controller (33) is also selected to cope with the general system stability issues. Therefore, we can select the controller according to the above three conditions to achieve better control effects.

#### 4.1. Control in Case 1

For the time-invariant constraint control, to guarantee the position constraints  $|q| < k_c = [0.24, 0.24]^T$  and to make the reference trajectory meet  $|x_d| \leq X_1$ , we select  $X_1 = [0.14, 0.14]^T$ , according to Assumption 4, the constraint boundary of the position tracking error is  $k_q = k_c - X_1 = [0.1, 0.1]^T$ . The parameters of the robotic tracking control system are selected as  $k_{11} = k_{12} = 1.8$ , and  $K_2 = \text{diag}(20, 20)$ .

The simulation results of time-invariant constraint control based on improved logarithmic barrier function for a two-degree robot are shown in Figures 1–4. The performance curve and error curve of the robotic system's position vector tracking desired targets are described in Figures 1 and 2. The error curves of the joint velocity vector of the robotic system tracking desired targets  $\alpha$  are given in Figure 3. Figure 4 depicts the control inputs of the two robotic arms.

Observing Figures 1 and 2, we can see that when the constraint boundary  $k_q$  is altered into a time-invariant situation and the improved logarithmic barrier function-based control approach without compensation for unknown terms of the robotic system (14), the control performance can still be accepted. The simulation effects evidence the universality of the presented improved logarithmic BLF (1), which can handle both systems with time-varying constraint requirements and systems with time-invariant constraint requirements. It is clear from Figures 1 and 2 that the position vector of joints 1 and 2 is successful in tracking the desired targets, although the tracking errors of the joints fluctuate a little bit around zero. Further, despite the controller not compensating for the system's uncertain terms, the position errors still do not violate the constrained boundary conditions  $k_{q1}$  and  $k_{q2}$ . In Figure 3, in the initial time, the errors of the joint velocity vector of the robotic system tracking desired targets  $\alpha$  are of a larger order of magnitude since the desired trajectory is required to be tracked as soon as possible, which needs a large initial desired velocity. The control inputs of the two robotic arms are depicted in Figure 4. In the initial stage, large

control inputs are required to ensure convergence of velocity errors and avoid position tracking errors exceeding boundaries.

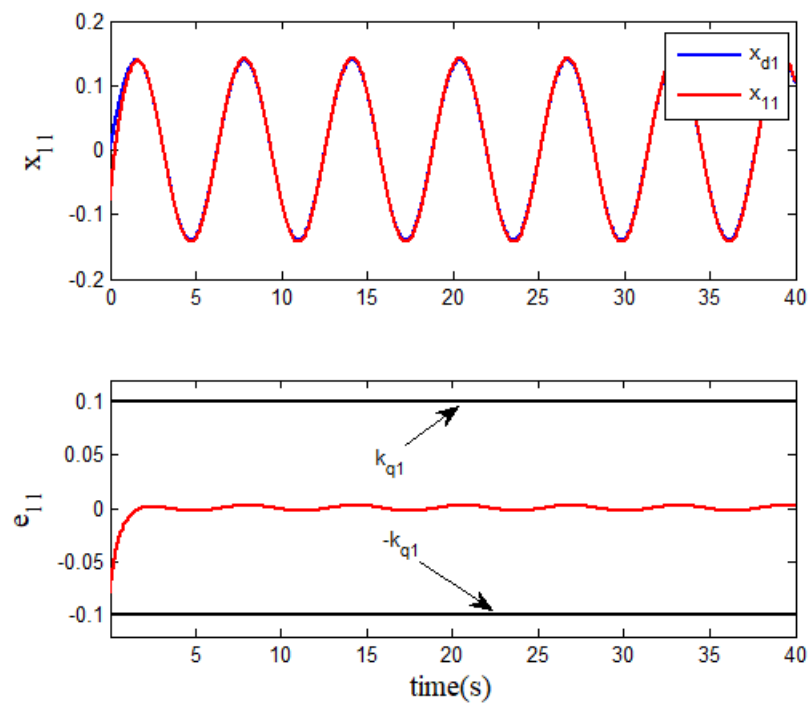


Figure 1. Tracking performance and error of joint 1 (first case).

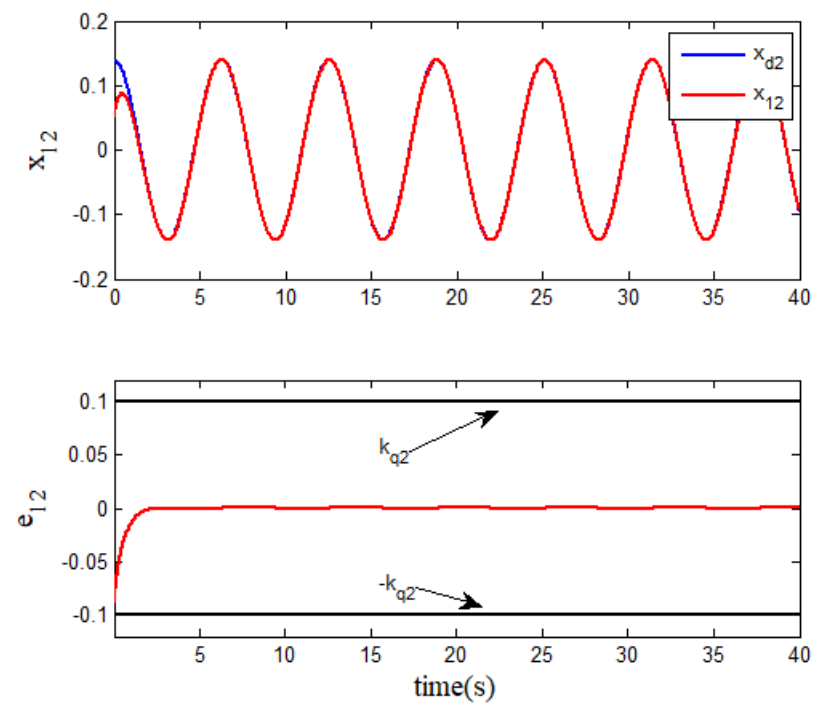


Figure 2. Tracking performance and error of joint 2 (first case).

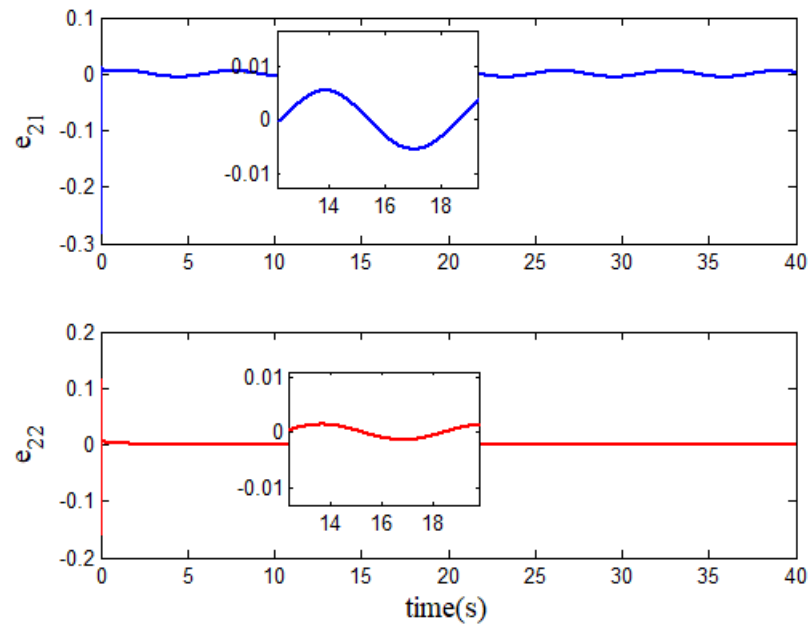


Figure 3. The velocity tracking errors (first case).

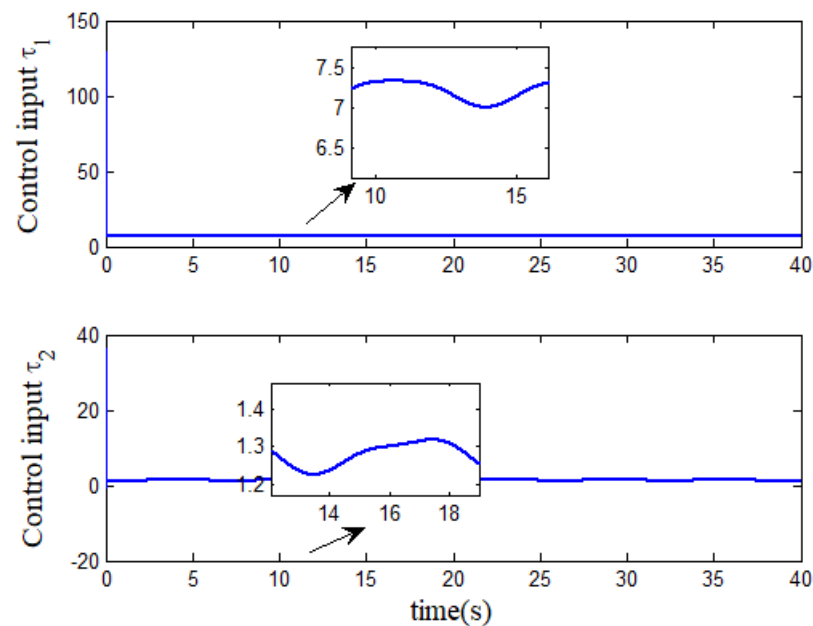


Figure 4. The control inputs of the two robotic arms (first case).

#### 4.2. Control in Case 2

For the time-variant constraint control of the robotic system, in order to ensure position constraints  $|q| < k_c(t) = [0.24 + 0.05 \cos(t), 0.24 + 0.05 \sin(t)]^T$  and to make the reference trajectory meet  $|x_d| \leq X_1$ , we select  $X_1 = [0.14, 0.14]^T$ , according to Assumption 4, the constraint boundary of the position tracking error is  $k_q(t) = k_c(t) - X_1 = [0.1 + 0.05 \cos(t), 0.1 + 0.05 \sin(t)]^T$ . The parameters of the robot tracking control system are set as  $k_{11} = k_{12} = 1.8$  and  $K_2 = \text{diag}(20, 20)$ , the observer parameter is chosen as  $k_f = \text{diag}(20, 20)$ .

The simulation results of time-variant constraint control by using an improved logarithmic barrier function for a two-link robot are given in Figures 5–9. The position-tracking performance of the robotic arms as well as corresponding tracking errors are depicted in Figures 5 and 6. Figure 7 describes the joint velocity vector's tracking error of the robotic

arms tracking desired targets  $\alpha$ . Figure 8 gives the control inputs of the robot with two degrees. The unknown terms of the system and estimations are described in Figure 9.

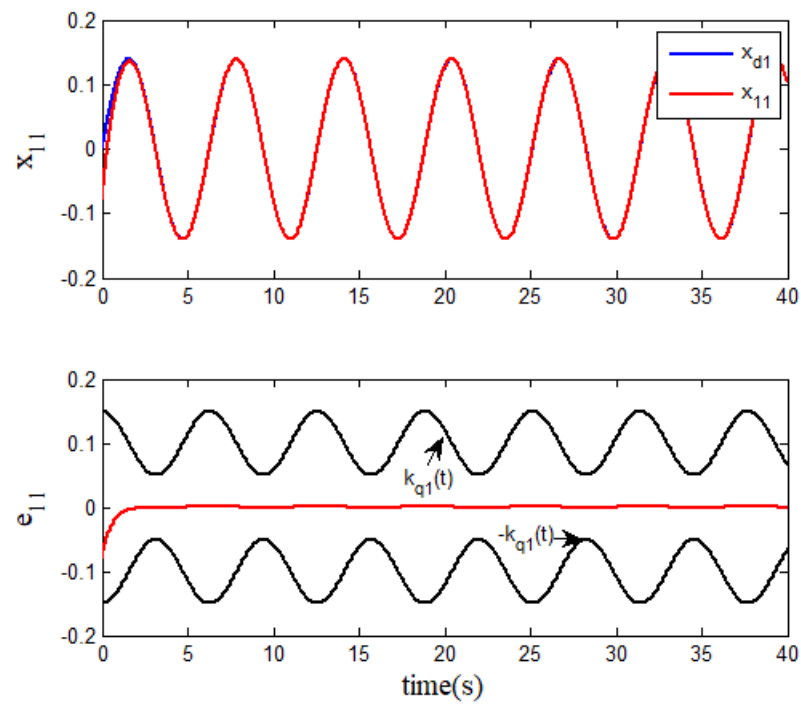


Figure 5. Tracking performance and error of joint 1 (second case).

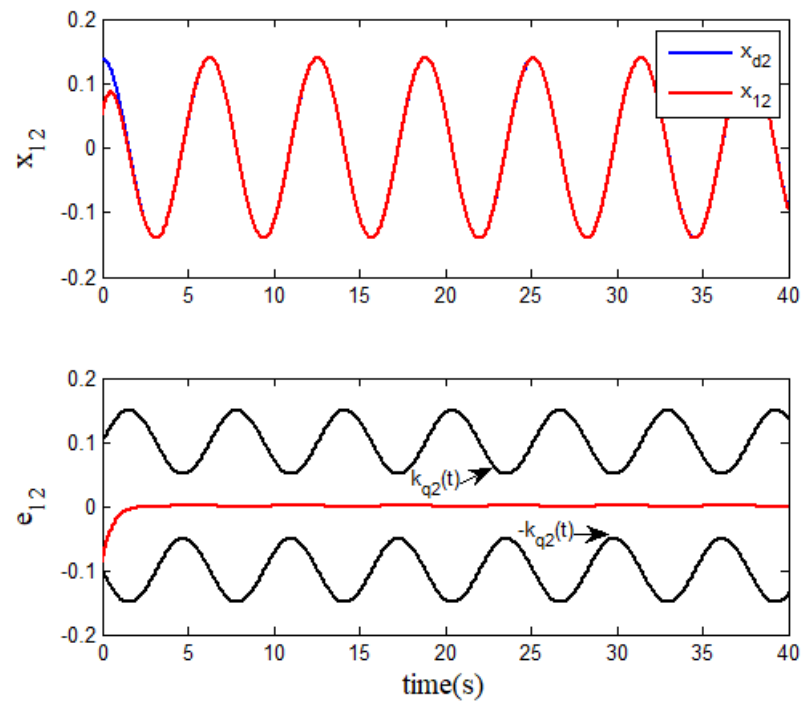


Figure 6. Tracking performance and error of joint 2 (second case).

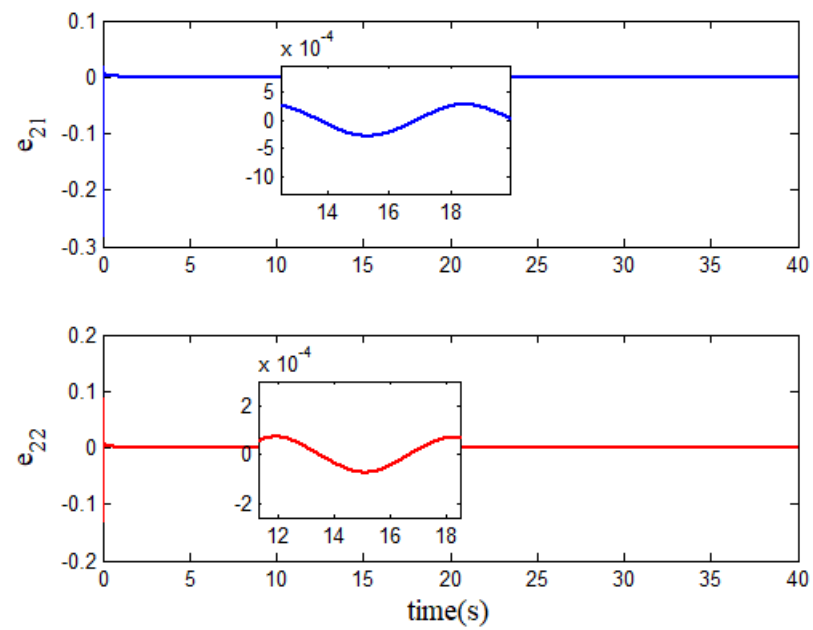


Figure 7. The velocity tracking errors (second case).

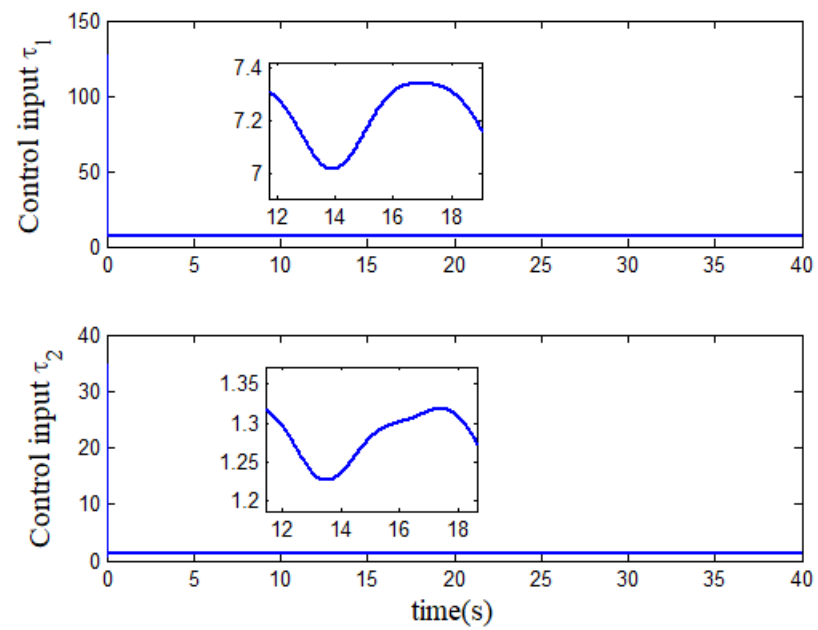
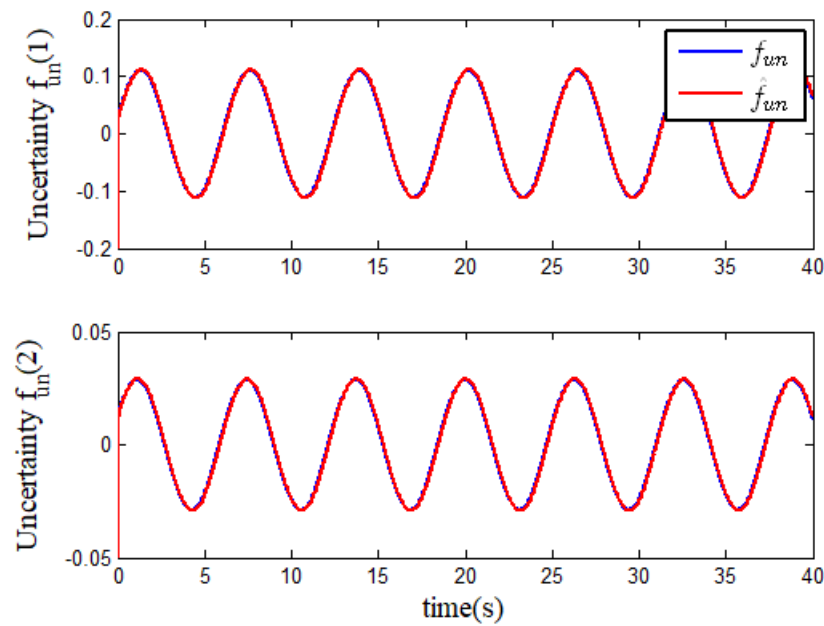


Figure 8. The control inputs of the two robotic arms (second case).



**Figure 9.** Uncertain term and estimation (second case).

Observing the simulation results about the time-variant constraint requirements of the robotic system in the second case, it can be seen that the improved time-variant logarithmic barrier function-based controllers (21) and (33) are feasible. Considering the simulation effects of Case 1 and Case 2 comprehensively, we arrive at the conclusion that the tracking method presented in this work is applicable to both systems subject to time-variant constraint requirements and systems subject to time-invariant constraint requirements. Next, we perform further analysis of the simulation effects. It is learned from Figures 1, 2, 5 and 6 that the position tracking precision of Case 2 is higher than that of Case 1. Meanwhile, the time-variant position constraint boundaries  $k_q(t)$  are always met. By comprehensively observing the simulation effects in Figures 3 and 7, it can be seen that the order of magnitude of the velocity tracking error  $e_2$  of Case 2 is significantly smaller than that of Case 1. The inputs of the robotic arm under the time-variant constraint and time-invariant constraint control strategies are basically similar. The evolution curves of the unknown terms  $f_{un}$  and estimations  $\hat{f}_{un}$  are given in Figure 9, and the observation effect is satisfactory.

#### 4.3. Control in Case 3

In order to verify the method is successful in dealing with the tracking control issue of the unconstrained system, we set the constraint boundary to infinite as  $k_{q1}(t) = k_{q2}(t) = 10^8$ . In addition, the traditional logarithmic time-varying barrier function is introduced into Case 3 to complete the comparative simulation [43]. However, when the constraint boundary is set as  $k_{q1}(t) = k_{q2}(t) = 10^8$ , the time-varying barrier function (3) and its derivative (6) are zero in [43]. Therefore, this does not satisfy the Lyapunov stability theory. In Case 3, the controller in [43] is only used in simulation, and the parameters of the two controllers are set to be the same. The parameters of the robot tracking control system are set as  $k_{11} = k_{12} = 8$  and  $K_2 = \text{diag}(30, 30)$ , and the observer parameter is chosen as  $k_f = \text{diag}(20, 20)$ .

The simulation results when the tracking error constraint boundary is set to  $k_{q1}(t) = k_{q2}(t) = 10^8$  are shown in Figures 10–13. Observing the simulation results, we can see that the improved time-variant logarithmic barrier function-based controllers (21) and (33) are feasible in dealing with tracking control of the unconstrained system. In addition, when we set the constraint boundary to be  $k_{q1}(t) = k_{q2}(t) = 10^8$ , the traditional BLF in [43] also ensures that the tracking control is successful, although it does not meet the Lyapunov stability theory. From Figures 10 and 11, it can be seen that the two controllers have similar tracking effects due to the same virtual control law and the same parameters selected.

However, the velocity tracking error and control input have significant shake at the initial moment in Figures 12 and 13. In addition, it can be seen from the simulation results of the three cases that the initial control input increases sharply due to the large position tracking error and the fact that the tracking error is very close to the constraint boundary. This phenomenon can easily lead to the failure of control tasks and damage to actuators. In order to ensure the smooth progress of robot tracking control tasks, the problem of input saturation will be further studied in our future articles.

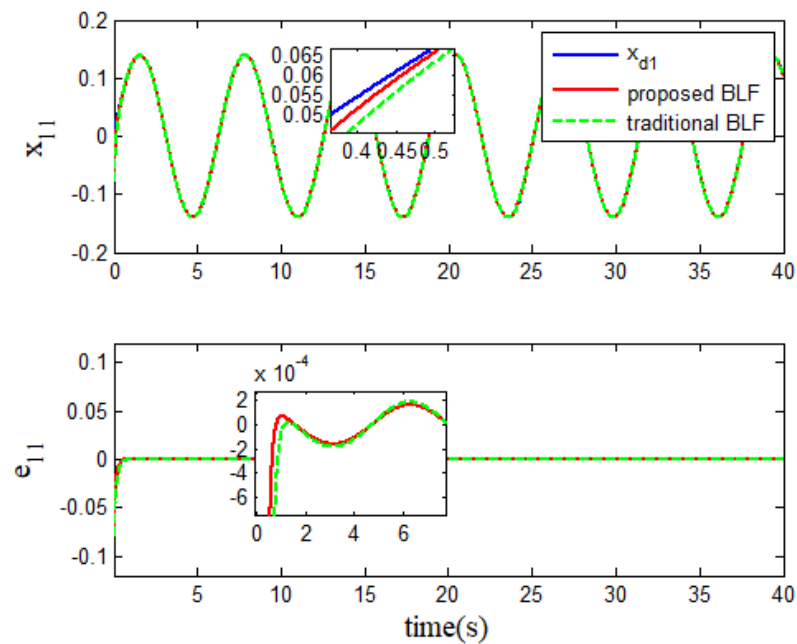


Figure 10. Tracking performance and error of joint 1 (third case).

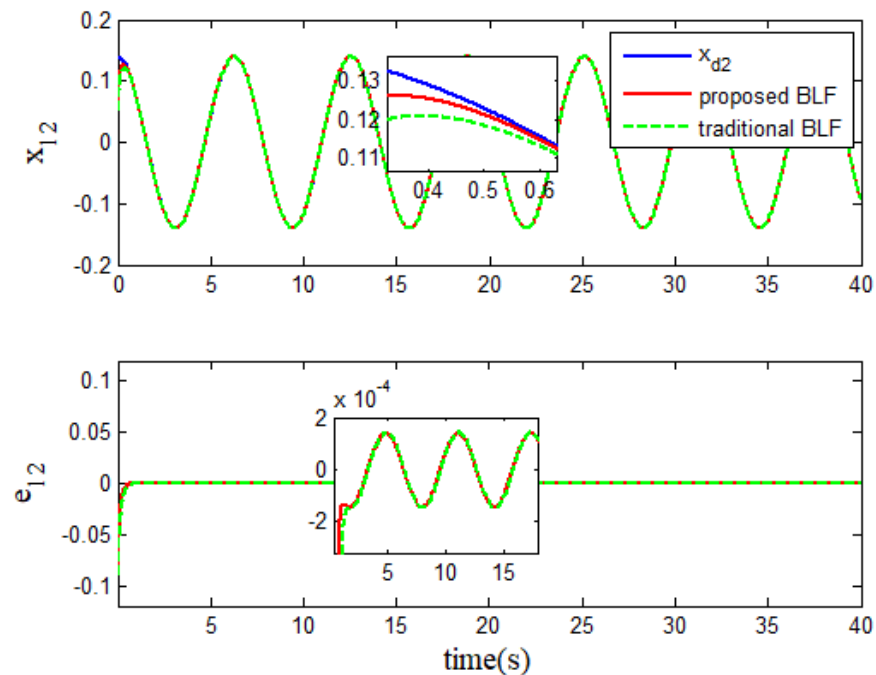


Figure 11. Tracking performance and error of joint 2 (third case).

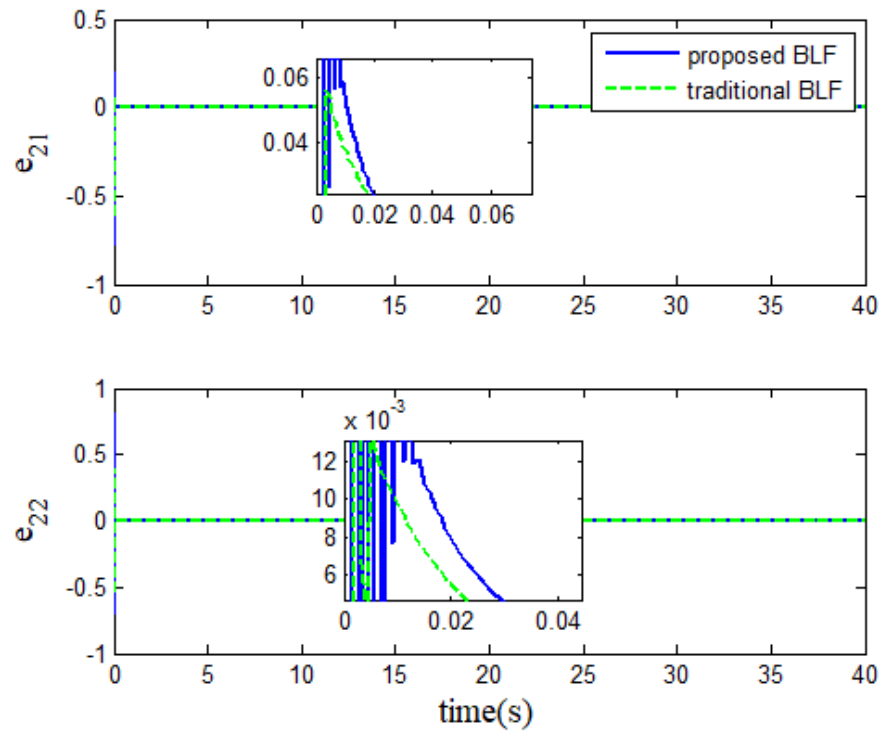


Figure 12. The velocity tracking errors (third case).

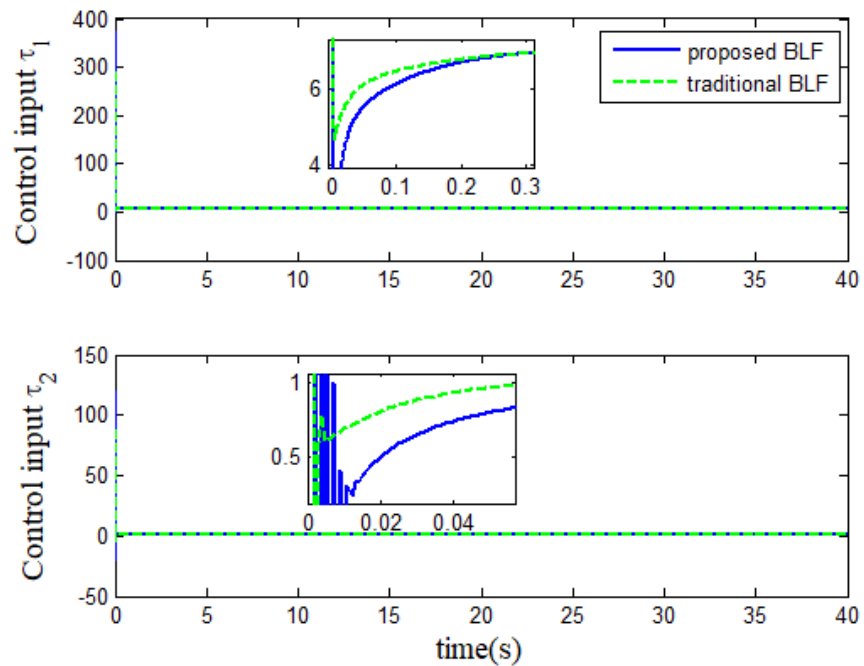


Figure 13. The control inputs of the two robotic arms (third case).

## 5. Conclusions and Future Research

In this work, by developing an improved universal logarithmic barrier function for the first time to deal with symmetric time-variant and time-invariant state constraints of the system and system without state-constrained requirements, the adaptive constraint control approach is presented for trajectory tracking problems for the n-link robotic system with system uncertain terms. The presented algorithm with the improved universal logarithmic BLF is a general one that is not only applicable to systems with constrained needs but also

to systems without constrained needs. And the corresponding Theorem on the proposed barrier function is also provided to prove the stability of the robotic system. An observer is led into estimating and compensating for the uncertain terms of the system. We indicate, from the results of three simulation cases, that the robotic system's position error vector can trend to zero asymptotically with acceptable accuracy.

In the future, we will change the symmetric logarithmic BLF proposed in this paper to an asymmetric one. The time-varying logarithmic barrier function proposed for the first time in this article is in a symmetric form; however, when the constraint boundary of the state becomes asymmetric, the control schemes based on the proposed barrier function will be useless. Although the barrier function in this article has the advantage of handling unconstrained systems compared to existing barrier functions, we still need to improve the barrier function in this article to handle asymmetric constraint problems. Moreover, the input saturation phenomenon often occurs in barrier function-based control tasks. In order to address the adverse effects of actuator saturation on control, it is necessary to introduce saturation control technology into robot constraint control.

**Author Contributions:** Conceptualization, methodology, software, validation, resources, writing—original draft preparation, visualization, and funding acquisition, T.Z.; formal analysis, investigation, data curation, writing—review and editing, supervision, and project administration, J.Z. All authors have read and agreed to the published version of the manuscript.

**Funding:** This research was funded by the Start-up Fee for Scientific Research of High-level Talents in 2022 under Grant Nos. WGKQ2022006 and WGKQ2022052 and the Scientific Research Projects of Universities in Anhui Province under Grant No. 2022AH051674.

**Institutional Review Board Statement:** Not applicable.

**Informed Consent Statement:** Not applicable.

**Data Availability Statement:** All data utilized to support the findings of this work are contained in the paper.

**Conflicts of Interest:** The authors declare no conflict of interest.

## References

1. Wang, L.; Chen, G.; Wang, X.; Tang, W.K.S. Controllability of networked mimo systems. *Automatica* **2016**, *69*, 405–409. [[CrossRef](#)]
2. Liu, L.; Tian, S.; Xue, D.; Zhang, T.; Chen, Y.; Zhang, S. A Review of Industrial MIMO Decoupling Control. *Int. J. Control Autom. Syst.* **2019**, *17*, 1246–1254. [[CrossRef](#)]
3. Ji, R.; Li, D.; Ma, J.; Ge, S.S. Saturation-Tolerant Prescribed Control of MIMO Systems With Unknown Control Directions. *IEEE Trans. Fuzzy Syst.* **2022**, *30*, 5116–5127. [[CrossRef](#)]
4. Tang, F.; Niu, B.; Wang, H.; Zhang, L.; Zhao, X. Adaptive Fuzzy Tracking Control of Switched MIMO Nonlinear Systems With Full State Constraints and Unknown Control Directions. *IEEE Trans. Circuit Syst. II Express Briefs* **2022**, *69*, 2912–2916. [[CrossRef](#)]
5. Yang, T.; Sun, N.; Fang, Y. Adaptive Fuzzy Control for a Class of MIMO Underactuated Systems With Plant Uncertainties and Actuator Deadzones: Design and Experiments. *IEEE Trans. Cybern.* **2022**, *52*, 8213–8226. [[CrossRef](#)]
6. Homaeinezhad, M.R.; Yaqubi, S.; Gholyan, H.M. Control of MIMO mechanical systems interacting with actuators through viscoelastic linkages. *Mech. Mach. Theory* **2020**, *147*, 103763. [[CrossRef](#)]
7. Hou, Q.; Ding, S. GPIO Based Super-Twisting Sliding Mode Control for PMSM. *IEEE Trans. Circuit Syst. II Express Briefs* **2021**, *68*, 747–751. [[CrossRef](#)]
8. Cao, J.; Xie, S.Q.; Das, R. MIMO Sliding Mode Controller for Gait Exoskeleton Driven by Pneumatic Muscles. *IEEE Trans. Control Syst. Technol.* **2018**, *26*, 274–281. [[CrossRef](#)]
9. Hu, X.; Hu, C.; Si, X.; Zhao, Y. Robust Sliding Mode-Based Learning Control for MIMO Nonlinear Nonminimum Phase System in General Form. *IEEE Trans. Cybern.* **2019**, *49*, 3793–3805. [[CrossRef](#)]
10. Bagheri, F.; Komurcugil, H.; Kukrer, O.; Guler, N.; Bayhan, S. Multi-Input Multi-Output-Based Sliding-Mode Controller for Single-Phase Quasi-Z-Source Inverters. *IEEE Trans. Ind. Electron.* **2020**, *67*, 6439–6449. [[CrossRef](#)]
11. Sui, S.; Tong, S. Finite-Time Fuzzy Adaptive PPC for Nonstrict-Feedback Nonlinear MIMO Systems. *IEEE Trans. Cybern.* **2023**, *53*, 732–742. [[CrossRef](#)]
12. He, W.; Kong, L.; Dong, Y.; Yu, Y.; Yang, C.; Sun, C. Fuzzy Tracking Control for a Class of Uncertain MIMO Nonlinear Systems With State Constraints. *IEEE Trans. Syst. Man Cybern. Syst.* **2019**, *49*, 543–554. [[CrossRef](#)]
13. Kadri, M.B. Model-Free Fuzzy Adaptive Control for MIMO Systems. *Arab. J. Sci. Eng.* **2017**, *42*, 2799–2808. [[CrossRef](#)]

14. Zeng, Z.G.; Zheng, W.X. Multistability of neural networks with time-varying delays and concave-convex characteristics. *IEEE Trans. Neural Netw. Learn. Syst.* **2012**, *23*, 293–305. [[CrossRef](#)] [[PubMed](#)]
15. Zeng, Z.G.; Zheng, W.X. Multistability of two kinds of recurrent neural networks with activation functions symmetrical about the origin on the phase plane. *IEEE Trans. Neural Netw. Learn. Syst.* **2013**, *24*, 1749–1762. [[CrossRef](#)] [[PubMed](#)]
16. Jin, Q.; Wang, H.; Su, Q.; Jiang, B.; Liu, Q. A novel optimization algorithm for MIMO Hammerstein model identification under heavy-tailed noise. *Isa Trans.* **2018**, *72*, 77–91. [[CrossRef](#)]
17. Wallam, F.; Tan, C.P. Output feedback Cross-Coupled Nonlinear PID based MIMO control scheme for Pressurized Heavy Water Reactor. *J. Frankl. Inst.* **2019**, *356*, 8012–8048. [[CrossRef](#)]
18. Lee, H.; Snyder, S.; Hovakimyan, N.  $\mathcal{L}_1$  Adaptive Output Feedback Augmentation for Missile Systems. *IEEE Trans. Aerosp. Electron. Syst.* **2018**, *54*, 680–692. [[CrossRef](#)]
19. Tong, S.; Li, Y. Adaptive Fuzzy Output Feedback Control of MIMO Nonlinear Systems With Unknown Dead-Zone Inputs. *IEEE Trans. Fuzzy Syst.* **2013**, *21*, 134–146. [[CrossRef](#)]
20. Nguyen, C.H.; Leonessa, A. Adaptive Predictor-Based Output Feedback Control for a Class of Unknown MIMO Linear Systems. *J. Nonlinear Sci.* **2017**, *27*, 1257–1290. [[CrossRef](#)]
21. Li, Y.; Li, K.; Tong, S. Finite-Time Adaptive Fuzzy Output Feedback Dynamic Surface Control for MIMO Non-strict Feedback Systems. *IEEE Trans. Fuzzy Syst.* **2019**, *27*, 96–110. [[CrossRef](#)]
22. Shi, W. Adaptive Fuzzy Output-Feedback Control for Nonaffine MIMO Nonlinear Systems With Prescribed Performance. *IEEE Trans. Fuzzy Syst.* **2021**, *29*, 1107–1120. [[CrossRef](#)]
23. Dimanidis, I.S.; Bechlioulis, C.P.; Rovithakis, G.A. Output Feedback Approximation-Free Prescribed Performance Tracking Control for Uncertain MIMO Nonlinear Systems. *IEEE Trans. Autom. Control* **2020**, *65*, 5058–5069. [[CrossRef](#)]
24. Sui, S.; Xu, H.; Tong, S.; Chen, C.L.P. Prescribed Performance Fuzzy Adaptive Output Feedback Control for Nonlinear MIMO Systems in a Finite Time. *IEEE Trans. Fuzzy Syst.* **2022**, *30*, 3633–3644. [[CrossRef](#)]
25. Bikas, L.N.; Rovithakis, G.A. Prescribed Performance Tracking of Uncertain MIMO Nonlinear Systems in the Presence of Delays. *IEEE Trans. Autom. Control* **2023**, *68*, 96–107. [[CrossRef](#)]
26. Wang, J.; Li, R.; Zhang, G.; Wang, P.; Guo, S. Continuous sliding mode iterative learning control for output constrained MIMO nonlinear systems. *Inf. Sci.* **2021**, *556*, 288–304. [[CrossRef](#)]
27. Jin, X. Adaptive Fixed-Time Control for MIMO Nonlinear Systems With Asymmetric Output Constraints Using Universal Barrier Functions. *IEEE Trans. Autom. Control* **2019**, *64*, 3046–3053. [[CrossRef](#)]
28. Liu, Y.-J.; Gong, M.; Liu, L.; Tong, S.; Chen, C.L.P. Fuzzy Observer Constraint Based on Adaptive Control for Uncertain Nonlinear MIMO Systems With Time-Varying State Constraints. *IEEE Trans. Cybern.* **2021**, *51*, 1380–1389. [[CrossRef](#)]
29. Qiu, J.; Sun, K.; Rudas, I.J.; Gao, H. Command Filter-Based Adaptive NN Control for MIMO Nonlinear Systems With Full-State Constraints and Actuator Hysteresis. *IEEE Trans. Cybern.* **2020**, *50*, 2905–2915. [[CrossRef](#)]
30. Wu, L.-B.; Park, J.H.; Xie, X.-P.; Liu, Y.-J. Neural Network Adaptive Tracking Control of Uncertain MIMO Nonlinear Systems With Output Constraints and Event-Triggered Inputs. *IEEE Trans. Neural Netw. Learn. Syst.* **2021**, *32*, 695–707. [[CrossRef](#)]
31. Li, M.; Li, Y.; Ge, S.S.; Lee, T.H. Adaptive Control of Robotic Manipulators With Unified Motion Constraints. *IEEE Trans. Syst. Man Cybern. Syst.* **2017**, *47*, 184–194. [[CrossRef](#)]
32. Ouyang, Y.; Dong, L.; Sun, C. Critic Learning-Based Control for Robotic Manipulators With Prescribed Constraints. *IEEE Trans. Cybern.* **2022**, *52*, 2274–2283. [[CrossRef](#)] [[PubMed](#)]
33. Zhao, K.; Song, Y. Neuroadaptive Robotic Control Under Time-Varying Asymmetric Motion Constraints: A Feasibility-Condition-Free Approach. *IEEE Trans. Cybern.* **2020**, *50*, 15–24. [[CrossRef](#)] [[PubMed](#)]
34. Tang, Z.-L.; Ge, S.S.; Tee, K.P.; He, W. Adaptive neural control for an uncertain robotic manipulator with joint space constraints. *Int. J. Control* **2016**, *89*, 1428–1446. [[CrossRef](#)]
35. Zhang, S.; Dong, Y.; Ouyang, Y.; Yin, Z.; Peng, K. Adaptive Neural Control for Robotic Manipulators With Output Constraints and Uncertainties. *IEEE Trans. Neural Netw. Learn. Syst.* **2018**, *29*, 5554–5564. [[CrossRef](#)]
36. He, W.; David, A.O.; Yin, Z.; Sun, C. Neural Network Control of a Robotic Manipulator With Input Deadzone and Output Constraint. *IEEE Trans. Syst. Man Cybern. Syst.* **2016**, *46*, 759–770. [[CrossRef](#)]
37. He, W.; Chen, Y.; Yin, Z. Adaptive Neural Network Control of an Uncertain Robot With Full-State Constraints. *IEEE Trans. Cybern.* **2016**, *46*, 620–629. [[CrossRef](#)]
38. Li, D.-P.; Li, D.-J. Adaptive Neural Tracking Control for an Uncertain State Constrained Robotic Manipulator With Unknown Time-Varying Delays. *IEEE Trans. Syst. Man Cybern. Syst.* **2018**, *48*, 2219–2228. [[CrossRef](#)]
39. Sun, W.; Su, S.-F.; Xia, J.; Nguyen, V.-T. Adaptive Fuzzy Tracking Control of Flexible-Joint Robots With Full-State Constraints. *IEEE Trans. Syst. Man Cybern. Syst.* **2019**, *49*, 2201–2209. [[CrossRef](#)]
40. Yang, C.; Huang, D.; He, W.; Cheng, L. Neural Control of Robot Manipulators With Trajectory Tracking Constraints and Input Saturation. *IEEE Trans. Neural Netw. Learn. Syst.* **2021**, *32*, 4231–4242. [[CrossRef](#)]
41. Yu, X.; He, W.; Li, H.; Sun, J. Adaptive Fuzzy Full-State and Output-Feedback Control for Uncertain Robots With Output Constraint. *IEEE Trans. Syst. Man Cybern. Syst.* **2021**, *51*, 6994–7007. [[CrossRef](#)]
42. Sun, W.; Wu, Y.; Lv, X. Adaptive Neural Network Control for Full-State Constrained Robotic Manipulator With Actuator Saturation and Time-Varying Delays. *IEEE Trans. Neural Netw. Learn. Syst.* **2022**, *33*, 3331–3342. [[CrossRef](#)]

43. Lu, S.-M.; Li, D.-P.; Liu, Y.-J. Adaptive Neural Network Control for Uncertain Time-Varying State Constrained Robotics Systems. *IEEE Trans. Syst. Man Cybern. Syst.* **2019**, *49*, 2511–2518. [[CrossRef](#)]
44. Liu, Y.-J.; Lu, S.; Tong, S. Neural Network Controller Design for an Uncertain Robot With Time-Varying Output Constraint. *IEEE Trans. Syst. Man Cybern. Syst.* **2017**, *47*, 2060–2068. [[CrossRef](#)]
45. Wu, Y.; Huang, R.; Wang, Y.; Wang, J. Adaptive tracking control of robot manipulators with input saturation and time-varying output constraints. *Asian J. Control* **2020**, *23*, 1476–1489. [[CrossRef](#)]
46. He, W.; Huang, H.; Ge, S.S. Adaptive Neural Network Control of a Robotic Manipulator With Time-Varying Output Constraints. *IEEE Trans. Cybern.* **2017**, *47*, 3136–3147. [[CrossRef](#)]
47. Liu, K.; Gao, H.; Ji, H.; Hao, Z. Adaptive Sliding Mode Based Disturbance Attenuation Tracking Control for Wheeled Mobile Robots. *Int. J. Control Autom. Syst.* **2020**, *18*, 1288–1298. [[CrossRef](#)]
48. Wang, Y.; Liu, K.; Ji, H. Adaptive robust fault-tolerant control scheme for spacecraft proximity operations under external disturbances and input saturation. *Nonlinear Dyn* **2022**, *108*, 207–222. [[CrossRef](#)]
49. Liu, K.; Wang, R.; Wang, X.; Wang, X. Anti-saturation adaptive finite-time neural network based fault-tolerant tracking control for a quadrotor UAV with external disturbances. *Aerosp. Sci. Technol.* **2021**, *115*, 106790. [[CrossRef](#)]
50. Yu, J.; Shi, P.; Dong, W.; Lin, C. Command Filtering-Based Fuzzy Control for Nonlinear Systems With Saturation Input. *IEEE Trans. Cybern.* **2017**, *47*, 2472–2479. [[CrossRef](#)]
51. Tee, K.P.; Ge, S.S.; Tay, E.H. Barrier Lyapunov Functions for the control of output-constrained nonlinear systems. *Automatica* **2009**, *45*, 918–927. [[CrossRef](#)]
52. Liang, X.; Wang, H.; Zhang, Y. Adaptive nonsingular terminal sliding mode control for rehabilitation robots. *Comput. Electr. Eng.* **2022**, *99*, 107718. [[CrossRef](#)]
53. Ames, A.D.; Xu, X.; Grizzle, J.W.; Tabuada, P. Control Barrier Function Based Quadratic Programs for Safety Critical Systems. *IEEE Trans. Autom. Control* **2017**, *62*, 3861–3876. [[CrossRef](#)]
54. Clark, A. Control barrier functions for stochastic systems. *Automatica* **2021**, *130*, 109688. [[CrossRef](#)]
55. Alan, A.; Molnar, T.G.; Das, E.; Ames, A.D.; Orosz, G. Disturbance Observers for Robust Safety-Critical Control With Control Barrier Functions. *IEEE Control Syst. Lett.* **2023**, *7*, 1123–1128. [[CrossRef](#)]

**Disclaimer/Publisher’s Note:** The statements, opinions and data contained in all publications are solely those of the individual author(s) and contributor(s) and not of MDPI and/or the editor(s). MDPI and/or the editor(s) disclaim responsibility for any injury to people or property resulting from any ideas, methods, instructions or products referred to in the content.